Hearing Research 293 (2012) 31–43

Contents lists available at SciVerse ScienceDirect

Hearing Research

journal homepage: www.elsevier.com/locate/heares

Review

Von Békésy and cochlear mechanics

Elizabeth S. Olson [a,*], Hendrikus Duifhuis [b], Charles R. Steele [c]

[a] OTO/HNS and Biomedical Engineering, Columbia University, NY, USA
[b] Faculty of Mathematics and Natural Sciences, University of Groningen, Netherlands
[c] Mechanical Engineering, Stanford University, CA, USA

ARTICLE INFO

Article history:
Received 14 February 2012
Received in revised form
17 April 2012
Accepted 23 April 2012
Available online 22 May 2012

ABSTRACT

Georg Békésy laid the foundation for cochlear mechanics, foremost by demonstrating the traveling wave that is the substrate for mammalian cochlear mechanical processing. He made mechanical measurements and physical models in order to understand that fundamental cochlear response. In this tribute to Békésy we make a bridge between modern traveling wave observations and those of Békésy, discuss the mechanical properties and measurements that he considered to be so important, and touch on the range of computational traveling wave models.

1. Introduction

Georg Békésy is the grand-daddy of experimental cochlear mechanics. He studied cochlear mechanics from many angles, in particular observations of basilar membrane motion, measurements of mechanical properties of cochlear components, and building and observing physical cochlear models. Fast-forwarding to the modern world, we are still very much reliant upon observations of intracochlear motion and measurements of mechanical properties in order to make further progress in understanding cochlear operation. Békésy got into cochlear mechanics via the phone company and that aspect of his career is shared with many auditory researchers.

At the time of Békésy's early measurements in the 1920s, the cochlear anatomy had been described and the concept of tonotopicity had been introduced. (In his Nobel lecture Békésy notes Corti, 1851; Kölliker, 1852; Hasse, 1867; Retzius, 1884; Kolmer, 1909; Held, 1926.) Helmholtz's theory of hearing (Helmholtz, 1885), based on the resonance of micro-components of the ear, was already out of favor due to the recognition that these micro-components were viscously damped and moreover, dynamically coupled to each other (Roaf, 1922; Wegel and Lane, 1924). Helmholtz's independent-oscillator theory was thus supplanted by "dynamical theories" in which the macromechanics of the cochlea were considered to work as whole. These theories were discussed in an article by Wever (1962) who noted that they fell into two groups, those preceding and those following Békésy's experimental observations of the cochlear traveling wave in 1928 (Békésy, 1928). Békésy's observations were pioneering, yet by being confined to unnaturally high stimulus levels and primarily post-mortem preparations, he left some of the best observations to his descendents: he did not observe the allure and power of cochlear emissions (Kemp, 1978), the beauty of cochlear amplification (Rhode, 1978), or witness the fantastic discovery of outer hair cell motility (Brownell et al., 1985) and the cloning of the prestin protein (Zheng et al., 2000).

In writing this chapter we begin with two topics that were part of Békésy's repertoire and are still going strong in modern measurements – observations of the cochlear traveling wave, and measurements of the mechanical properties of cochlear tissues. Békésy started out with measurements on quantitatively scaled physical models but came to realize that to properly understand the cochlea and address theories of its operation he should measure the pattern of motion in the cochlea. His subsequent documentation of the cochlear traveling wave is probably Békésy's most significant single contribution, and its observation in modern measurements of basilar membrane (BM) motion (reviewed in Robles and Ruggero, 2001), reticular lamina motion (Chen et al., 2011), intracochlear pressure close to the organ of Corti (Olson, 1999; Dong and Olson, 2008a), cochlear microphonic (Dallos and Cheatham, 1971; Schmiedt and Zwislocki, 1977) and auditory nerve (AN) responses (Kiang et al., 1965; Kim and Molnar, 1979; Van der Heijden and Joris, 2006) underscore this unifying feature of cochlear processing. Thus our first section will be a panorama of in vivo traveling wave observations made with modern tools.

In his experiments with physical models Békésy found that variations in BM stiffness led to qualitative differences in behavior,

* Corresponding author.
E-mail addresses: eao2004@columbia.edu (E.S. Olson), H.Duifhuis@rug.nl (H. Duifhuis), chasst@stanford.edu (C.R. Steele).

0378-5955/$ – see front matter © 2012 Elsevier B.V. All rights reserved.
doi:10.1016/j.heares.2012.04.017

with very compliant BMs giving rise to reflections and thus standing waves, and less compliant BMs giving rise to unidirectional traveling waves. In the introduction to the book describing his life's work, "Experiments in Hearing" Békésy wrote: "Perhaps the most significant measurement in relation to the operation of the cochlea is that of the volume elasticity of the basilar membrane." Thus, the macromechanical properties of cochlear tissues were recognized by Békésy as being of primary importance to an understanding of cochlear mechanical processing. For our second topic we concentrate on modern measurements of BM stiffness, and provide some instruction for going between measured quantities and cochlear computational models. Our last section touches on cochlear computational models, which build on the traveling wave framework discovered by Békésy, in order to explore modern questions. In these topics – traveling wave observations, measurements of macromechanical properties, and the synthesis provided by cochlear modeling – we hope to pay proper tribute to Békésy and his ongoing significance to our field.

2. Cochlear traveling wave

2.1. Tonotopic map

Békésy measured the cochlear traveling wave by opening up the cochlea widely, one turn at a time, and using a strobe light and microscope to observe the motion visually. He stimulated at high levels, directly to the oval window. He made observations on many animals – pages 502–509 of his book (Békésy, 1960) contain the menagerie of guinea pig, chicken, mouse, rat, cow and elephant and earlier in the book he reports measurements on human temporal bone. Because his techniques for observing were relatively invasive and the stimulus levels excessive, it is not clear whether his observations represent normal-passive mechanics, where "normal-passive" stands for a linear cochlea without active behavior. Fig. 1 shows the guinea pig map Békésy reported compared to the modern map determined with single-unit AN recordings (Greenwood, 1990). If Békésy's map were of normal-passive responses, one would expect a ~ half octave shift downward in frequency compared to the active/healthy map, thus we also present Békésy's results shifted upward by a half octave. This expectation is based on the well-documented observation that the peak of the response pattern shifts basally with increased stimulus level (decreasing degree of activity) and post mortem (reviewed in Robles and Ruggero, 2001). The expectation that AN and BM motion measurements would line up in a modern low-stimulus level measurement is a reasonable approximation, as will be discussed further below (Narayan et al., 1998). In Fig. 1 the shifted Békésy map differs from the neural map by ~ another half octave, or equivalently, by about 1 mm in distance. Overall, that seems quite good, and argues that Békésy's motion measurements were close to normal-passive. A further indication of his consistency is the peak frequency that is estimated from his measurement of guinea pig BM volume compliance at various longitudinal locations (Figs. 12–37 in his book, which is redrawn in our Fig. 8). When volume compliance and fluid density are known, a rough estimate of the place-frequency map can be calculated, as described in the "Scale models" section below. The result of this calculation is included in Fig. 1 and is in reasonable agreement with Békésy's direct measurement of the guinea pig cochlear map (Fig. 6).

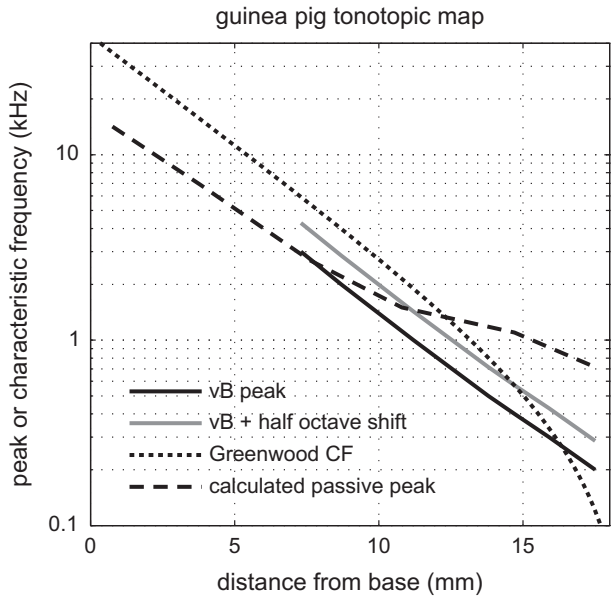

Fig. 1. Guinea pig tonotopic map from Békésy's BM displacement measurements and the same data shifted up 0.5 octave, compared to Greenwood's tonotopic map determined with AN recordings coupled to anatomical staining. Also shown is a theoretical estimate of the passive peak location using Békésy's BM compliance measurement.

2.2. Human – BM displacement

We introduce our panorama of traveling waves with Békésy's own measurements from the human cochlea, redrawn from Figs. 12–17(b) in his book and shown in our Fig. 2. Responses are shown for 200 Hz stimulation at four phases of the cycle. The characteristic traveling wave pattern is evident, with wavelength shortening as the wave travels toward the apex.

2.3. Gerbil – BM velocity

Our first two modern traveling waves are measurements in which the spatial pattern was actually sampled. The first measurement, in Fig. 3, is BM velocity from Ren (2002), made using a heterodyne laser vibrometer from Polytec (Waldbronn, Germany) coupled to a custom built microscope and used with a motorized translation stage for scanning. Ren measured the traveling wave pattern in gerbil over a ~1 mm extent, which was viewed through the round window opening. The spatial sampling distance was 2.5 μm. The responses were measured in vivo in an active cochlea. We show responses at two stimulus levels, 50 and 80 dB SPL, out of several in the original reference. The stimulus was a 16 kHz tone, which peaked within the explored region. Our figure is based on Ren's Fig. 1, in which the data were presented as amplitude, phase and as a response pattern at one time of the stimulus cycle. In our Fig. 3 we show the pattern at six times of stimulation by plotting [amplitude × cos(phase)], [amplitude × cos(phase + pi/6)] etc,

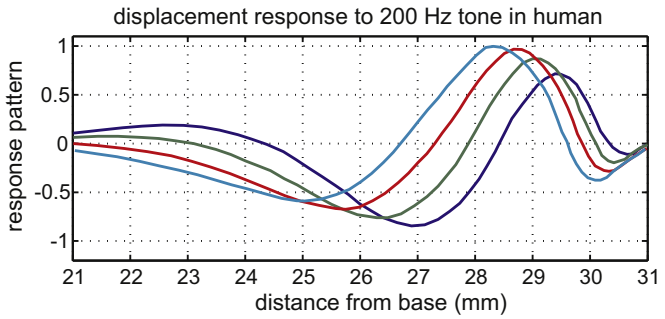

Fig. 2. BM displacement measured by Békésy in human, at four points of the stimulus cycle.

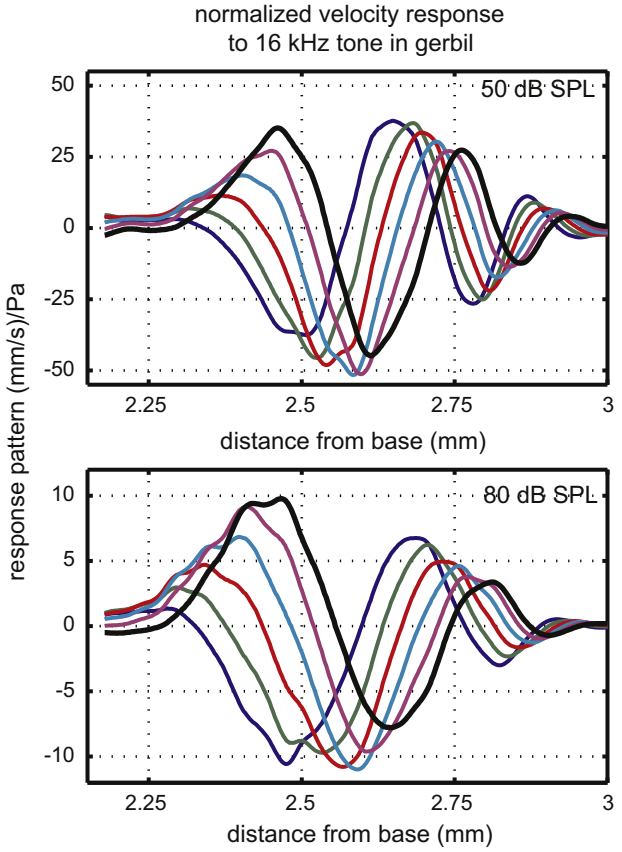

Fig. 3. BM velocity measured by Ren in gerbil. Amplitude and phase data are combined to give the response pattern at six points within half a stimulus cycle.

through a half cycle of stimulation (6 "snapshots"). Based on the tonotopic map (Müller, 1996) the basal gerbil cochlea maps an octave in ~1.5 mm, a value consistent with Ren's observations. Thus the explored 1 mm region would map between a half and a full octave. As in Békésy's observations, the wavelength shortened as the wave traveled toward the apex. Comparing the 50 and 80 dB SPL responses, the peak is further apical in the 50 dB result, thus cochlear activity allowed the wave to travel further before it peaked. Comparing the peaks, the normalized response is almost 4 times larger at 50 than at 80 dB SPL. The wavelength did not change much with level, but the wavelength at the peak was longer at 80 dB than 50 dB. The responses at these two levels show the trend and when the full range of SPLs reported in the original paper is considered the level-dependent differences are larger. The wavelength at the peak was much shorter (~20 times) than in Békésy's measurements in Fig. 2. One likely contribution to the difference is that the human measurements were made at 200 Hz, and the gerbil at 16 kHz. It is well known, and was noted by Békésy too, that higher frequencies evoke more localized, sharper responses. Also, as noted above, Békésy's preparations were likely not quite normal-passive. Finally, if Ren's measurements extended further basal, the 80 dB wavelength at the peak might prove to be longer than it appears in the limited view.

2.4. Cat — auditory nerve responses

Our second modern measurement is also an actual longitudinal sampling along the cochlea, and comes from single-unit AN recordings in cat by Van der Heijden and Joris (2006). In Fig. 4, the top three panels (A–C) are redrawn from their paper. Circles indicate the unit's characteristic frequency (CF). (CF is the frequency at which the neural threshold is minimum. Below we will also use the term CF to indicate the peak of the BM response at low-stimulus levels.) Fig. 4A shows the normalized amplitude obtained from the responses to tone complexes. These are amplitude versus frequency curves, with the different curves representing different ANs — and thus, different locations. Fig. 4B shows the corresponding phase curves. In Fig. 4C, the phase data are replotted as phase versus location with the different colors representing various stimulus frequencies. To explain how this is done: For example, to construct the 1 kHz curve (aqua, with arrow pointing to it), a vertical line is drawn at 1 kHz in Fig. 4B. Most of the ANs responded to 1 kHz stimulation (their responses pass through the vertical line), and in Fig. 4C the responses to 1 kHz are plotted versus location by transforming each AN's CF to location, using the tonotopic map (Greenwood, 1990) (bottom axis of C). The bottom x-axis of Fig. 4C indicates distances from 0 to 10 mm from the apex in the cat, whose cochlear length is ~20 mm. In the top x-axis of Fig. 4C the CF of the location is noted. In the phase data of Fig. 4B there is a question of how much neural and middle ear delays contribute, but in Fig. 4C these delays cancel out with the assumption that the delays were the same for all the AN fibers. The authors plotted the data in Fig. 4C as distance from the apex and in Fig. 4D the Fig. 4C curve corresponding to 1 kHz stimulation is replotted versus distance "toward" the apex (solid line), which reverses its orientation to the more familiar view. Also in Fig. 4D is an amplitude plot for 1 kHz stimulation (dashed curve), drawn from the amplitude data in Fig. 4A in a similar manner. In Fig. 4E we show the traveling wave pattern for 1 kHz stimulation at six times through a half cycle of stimulation — a "stroboscopic" view. These AN responses are not part of the mechanical traveling wave, but are a modified read-out of the wave, since mechanical/electrical and chemical processes occurring between the BM and the AN responses shaped these responses (e.g., Kidd and Weiss, 1990; Guinan et al., 2005). As an aside, theories of AN processing incorporate the neural timing that results from the mechanical traveling wave (e.g., Joris et al., 2006; Carney, 1994). The wavelength is about 2 mm at the peak, reasonably in line with Békésy's in Fig. 2 and longer than the high frequency region in gerbil from Fig. 3.

Our final two examples of traveling wave behavior were not spatial measurements; they were measurements at one place, which we have combined with the tonotopic map and the concept of scaling symmetry (Zweig, 1976, 1991) to extrapolate a traveling wave pattern. Scaling symmetry is based on the observation that when BM motion was measured at two locations (x_1 or x_2), the responses as a function of frequency (call them $R(f,x_1)$ and $R(f,x_2)$) were almost identical if each was plotted as a function of $f \div \mathrm{CF}(x)$. In other words, the response that we think of as depending on the two variables, frequency and location, depends more concisely on the single variable $f/\mathrm{CF}(x)$.

$$R(f,x) \rightarrow R\left(\frac{f}{\mathrm{CF}(x)}\right) \tag{1}$$

This symmetry of response was referred to by Zweig as scaling symmetry, expressed in Eq. (1). (Zweig noted that the size of the response varied with location and here we do not include that detail.) Armed with this relationship, once we have the response at one location and many frequencies (the usual modern measurement, left side of Eq. (2)) and the tonotopic map of the cochlea $\mathrm{CF}(x)$, we can find the response at one frequency and many locations.

$$R\left(\frac{f}{\mathrm{CF}\left(x_{\mathrm{fixed}}\right)}\right) = R\left(\frac{f_{\mathrm{fixed}}}{\mathrm{CF}(x)}\right) \tag{2}$$

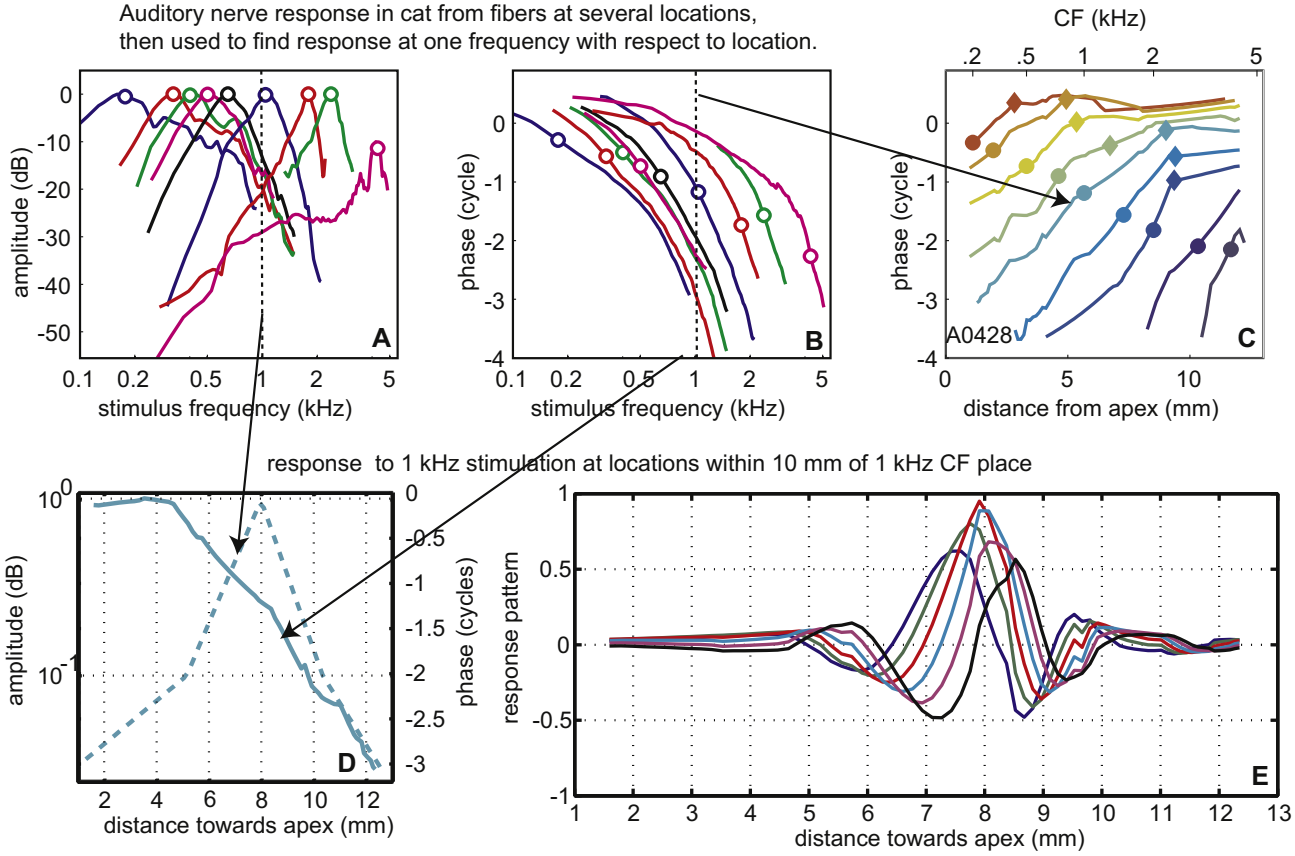

Fig. 4. Auditory nerve responses measured by Van der Heijden and Joris in the cat, and their analysis to find traveling wave patterns. (A) Response amplitudes from nine ANs as a function of frequency and (B) corresponding phases. (C) Each curve shows phase for stimulation at one frequency as a function of location, and is derived from data in B. The phase versus location response for 1 kHz stimulation is emphasized – dashed line at 1 kHz in B, aqua curve in C. *x*-axis plotted as distance from apex. (D) Amplitude and phase of the response to 1 kHz stimulation, with *x*-axis reversed to distance toward apex. (E) Traveling wave patterns derived from D.

Fortunately, tonotopic maps exist for many species, often derived from AN response measurements followed by staining and tracing of the characterized AN fiber (Greenwood, 1990; Müller, 1996; Müller et al., 2010), and sometimes from measurements of local cochlear microphonic (Schmiedt and Zwislocki, 1977) or locally induced damage (Eldredge et al., 1981).

As it happens, the mammalian tonotopic map is known to be approximately exponential: $\mathrm{CF} = f_0 e^{-x/a}$, where a is a constant, and in that case:

$$R\left(\frac{f}{\mathrm{CF}}\right) = R\left(\frac{f}{f_0 e^{-x/a}}\right) = R\left(\frac{f e^{x/a}}{f_0}\right) \tag{3}$$

Eq. (3) explains why the response curve plotted for one location as a function of log f looks the same as the response curve plotted for one frequency as a function of x. However, the concept of scaling symmetry does not rely on the form of the CF map, but simply on the similarity of the responses measured at different locations expressed in Eq. (1). To give a concrete example of how the conversion works, let's say we measured BM velocity over a wide range of frequencies at the location with 20 kHz low-level best frequency, which we equate to CF. We will put the responses in a table with the first column stimulus frequency/CF (the number that results from the division), the second column the response amplitude, and the third column the response phase relative to the cochlear input phase. (The phase reference can be stapes motion, or intracochlear pressure at the stapes. Often the input phase that is known is the ear canal pressure and in that case the phases should be corrected by subtracting the frequency-dependent phase corresponding to middle ear delay.) We want to know the response along the cochlear length to a given tone of frequency f_1. The response at a given CF's location to our f_1 is found by going to the look-up table's first column for the value corresponding to the value f_1/CF, and reading off response amplitude and phase from that row of the table, then going on to the next CF etc. This gives us R(CF) and the tonotopic map CF(x) is used to convert this to $R(x)$.

As Zweig pointed out, scaling symmetry is most accurate in the base and over a limited region (local-scaling symmetry). Accordingly, the last two examples are from the cochlear base and we plot $R(x)$ at a frequency that peaked within the region of the actual measurement.

2.5. Chinchilla – BM displacement

The first of these final two, Fig. 5, is a BM displacement measurement by Rhode (2007), using a phase-sensitive laser vibrometer that measures displacement (Cooper and Rhode, 1992). Rhode's data were from the mid-basal cochlea of chinchilla and the data in the upper two panels were from the 9 kHz best place. We show data taken at 30 and 70 dB SPL, a subset of those in the original paper. Rhode attributed the pronounced notches below 5 kHz to the middle ear and we used a smoothed version of the 70 dB data when calculating spatial patterns. The chinchilla middle ear delay (Ravicz et al., 2010) has been subtracted from the phase, which was originally referenced to ear canal pressure. In the

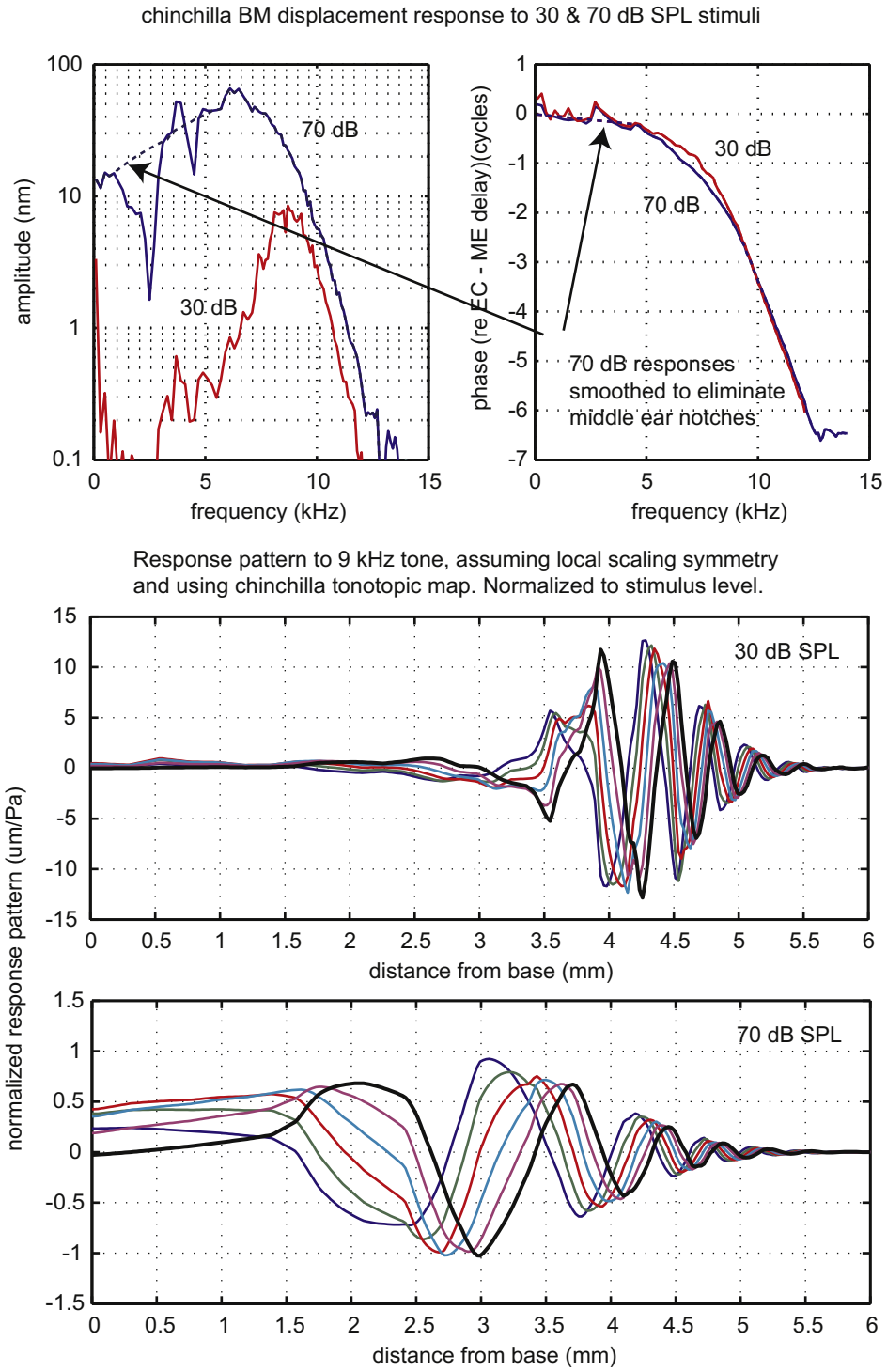

Fig. 5. Basilar membrane displacement measured by Rhode in chinchilla. Upper panels show amplitude and phase as a function of frequency. In the lower two panels the data are replotted as the response pattern, assuming scaling symmetry and using the tonotopic map.

bottom panels the frequency responses are recast as traveling wave responses, using the chinchilla cochlear map (Müller et al., 2010). Comparing the responses at the two levels, the trends apparent in Ren's results in Fig. 3 are even more pronounced – at 30 dB SPL the traveling wave peaks significantly further apical than it does at 70 dB SPL. The wavelength in the peak region is substantially longer at 70 than at 30 dB, about 1.5 mm compared to just over a half millimeter. However, the wavelength shortens similarly with distance at the two stimulus levels, an outcome that is prescribed by the overall similarity of the phases of the responses at the two levels. The normalized response peak is ~13 times larger at 30 than at 70 dB SPL. Comparing responses at the low-level best place, the normalized response at 30 dB is ~35 times larger than that at 70 dB. When the range of SPLs shown in the original paper is considered, at the CF the ratio of normalized responses differs by almost a factor of 1000. It is an important and

robust observation that in contrast to the dramatic level-dependent change in amplitude the phase shows only a subtle change. This observation led to the conclusion that cochlear amplification works by changing the resistance, not stiffness (e.g., Kolston, 2000).

2.6. Gerbil – pressure at the BM

Our final traveling wave example comes from measurements of pressure close to (~10 μm from) the BM in scala tympani, using fiber-optic based micro-pressure sensors that were developed for this purpose. Two stimulus levels, 50 and 80 dB SPL, are shown (Olson, 1999). As in the Rhode data just presented, the original data are in the top panels, amplitude and phase, and extrapolated traveling waves below. The extrapolation used the gerbil tonotopic map by Müller (1996). The phase reference was the intracochlear pressure measured in scala vestibuli near the stapes – the input pressure of the cochlea. The pressure measured close to the BM is tuned and nonlinear and the phase shows traveling wave accumulation. An obvious difference between the pressure and BM motion responses is the presence of a fairly high-level plateau at frequencies above the BF – this is attributed to the fast wave pressure (Peterson and Bogert, 1950; Olson, 2001; Yoon et al., 2011). In the traveling wave panels, the pressure at the BM exhibits the same trends as the BM motion seen above, with the peak occurring further apical and the wavelength shortening closer to the apex at the lower-stimulus level. Where the response peaks, the wavelength is ~0.4 mm at 50 dB SPL and about 0.8 mm at 80 dB SPL. The normalized response peak is ~3 times larger at 50 than at 80 dB SPL. Comparing responses at the low-level best place, the normalized response at 50 dB is almost 5 times larger than that at 80 dB. At locations apical to the peak, the response maintains a plateau of fast wave pressure. At 50 dB SPL the traveling wave superimposes small ripples on the fast wave plateau, but at 80 dB only the plateau is observed (Fig. 6).

The figures in this section document the ubiquity of Békésy's cochlear traveling wave in modern intracochlear measurements. They also underscore the tight connection between BM motion, pressure at the BM and AN responses, and reinforce the dynamical view of cochlear operation. The reports of Narayan et al. (1998) and Ruggero et al. (2000) documented the close similarity between BM motion and AN responses in the base of the chinchilla cochlea. An example of this important result is included in Fig. 7, with data redrawn from Fig. 2 of Ruggero et al. (2000).

We close this section with a caveat: The uniform view of the cochlea expressed in the concept of scaling symmetry is a reasonable approximation for the basal half of the cochlea, but is less accurate in apical regions. Kiang and colleagues (e.g., Kiang and Moxon, 1973) showed that the tuning curves of AN fibers with CFs < 3 kHz (close to half of the cochlear length in cat) were less sharply tuned than the higher CF fibers, with broadening primarily on the low frequency side. For CFs < 1 kHz, close to the cochlear apex, the AN tuning curves were often multi-lobed, an observation that does not have a counterpart in mechanical measurements in the apex. In this vein, the close correspondence between macromechanical motion and AN responses illustrated in Fig. 7 does not apply to the cochlear apex, where the mechanical tuning is less sharp than AN tuning, particularly on the low frequency side where the mechanical tuning is very broad (Dong and Cooper, 2006). These observations indicate that in the apical cochlea, micromechanical processing impacts the stereocilia differently than the BM, leading to a relatively nuanced correspondence between macromechanical motion and AN responses compared to more basal locations (Guinan et al., 2005). Techniques to measure micromechanical motion in vivo are advancing and we look forward to a more complete view of the relationship between BM motion, micromechanics and AN responses.

3. Mechanical properties

3.1. Scale models

A remarkable characteristic of Békésy was his ability to construct physical models that demonstrate key features of the cochlea's mechanical response. Since a life-sized model of the cochlea is difficult, he and many subsequent investigators, e.g. Cancelli et al. (1985), used models that were larger than life-size. Békésy (p. 406 in his book) realized that two dimensionless parameters must be preserved for a large model to preserve the correct response. His two parameters may be recombined as:

$$\gamma_1 = \frac{\sqrt{\mu/\rho\omega}}{L} \tag{4}$$

$$\gamma_2 = \frac{\pi\rho\omega^2\varepsilon}{L} \tag{5}$$

μ is the viscosity (Pa s), ρ is the density (kg/m^3), ω is the angular frequency (1/s), ε is the volume compliance m^2/Pa, and L is a characteristic length (m). In this form, γ_1 is the ratio of the viscous boundary layer thickness to L, and γ_2 is a ratio of inertia to stiffness. Setting $\gamma_2 = 1$ yields the relation between the local compliance of the partition and the frequency at which the partition would resonate in infinite fluid. In cochlear models this is not a resonant point, but it is an indicator of the transition to short wavelengths that occurs near the peak of the passive BM response. Thus, this simple calculation allows for a rough estimate of the passive cochlear map.

3.2. Compliance

As noted above, Békésy considered the stiffness of the cochlear partition to be the most significant measurement for understanding cochlear mechanics. Békésy measured compliance by isolating 1 mm sections of the cochlear partition by using agar to plug one side and by cutting back sequentially from the other side. Once a section was isolated, he applied a static pressures due to ~1 cm of water (corresponding to a pressure $\rho gh \sim 100$ Pa), and measured the BM area displacement, then he went on to the next section. The result was presented on p. 476 and 510 of his book as volume of displaced fluid (with 1 mm being the length of the longitudinal sections). This can be used to determine compliance or its inverse, stiffness. No one else to our knowledge has measured BM stiffness using Békésy's method, but stiffness has been measured using other methods by a number of groups. Two relatively early measurements were those of Gummer et al. (1981) and Miller (1985), in excised cochlea of guinea pig. Both of these used point stiffness measurements. Point stiffness has also been measured in gerbil (in vivo: Olson and Mountain (1994); excised cochlea: Naidu and Mountain (1998); excised hemi-cochlea, with subset in vivo: Emadi et al. (2004).) The experimental studies of Gummer et al. and Miller were analyzed using models of simple or complex beams, and Steele and colleagues did a detailed computer model of the stiffness of water buffalo BM (Steele, 1999), and more recently of gerbil (Kapuria et al., 2011). In vivo BM stiffness was found through a wide range of frequencies with combined pressure and motion measurements (Dong and Olson, 2009) and with pressure measurements and analysis (Olson, 2001).

In Fig. 8 we present macromechanical measures of stiffness, with a goal to relate diverse measurements and tie them to the

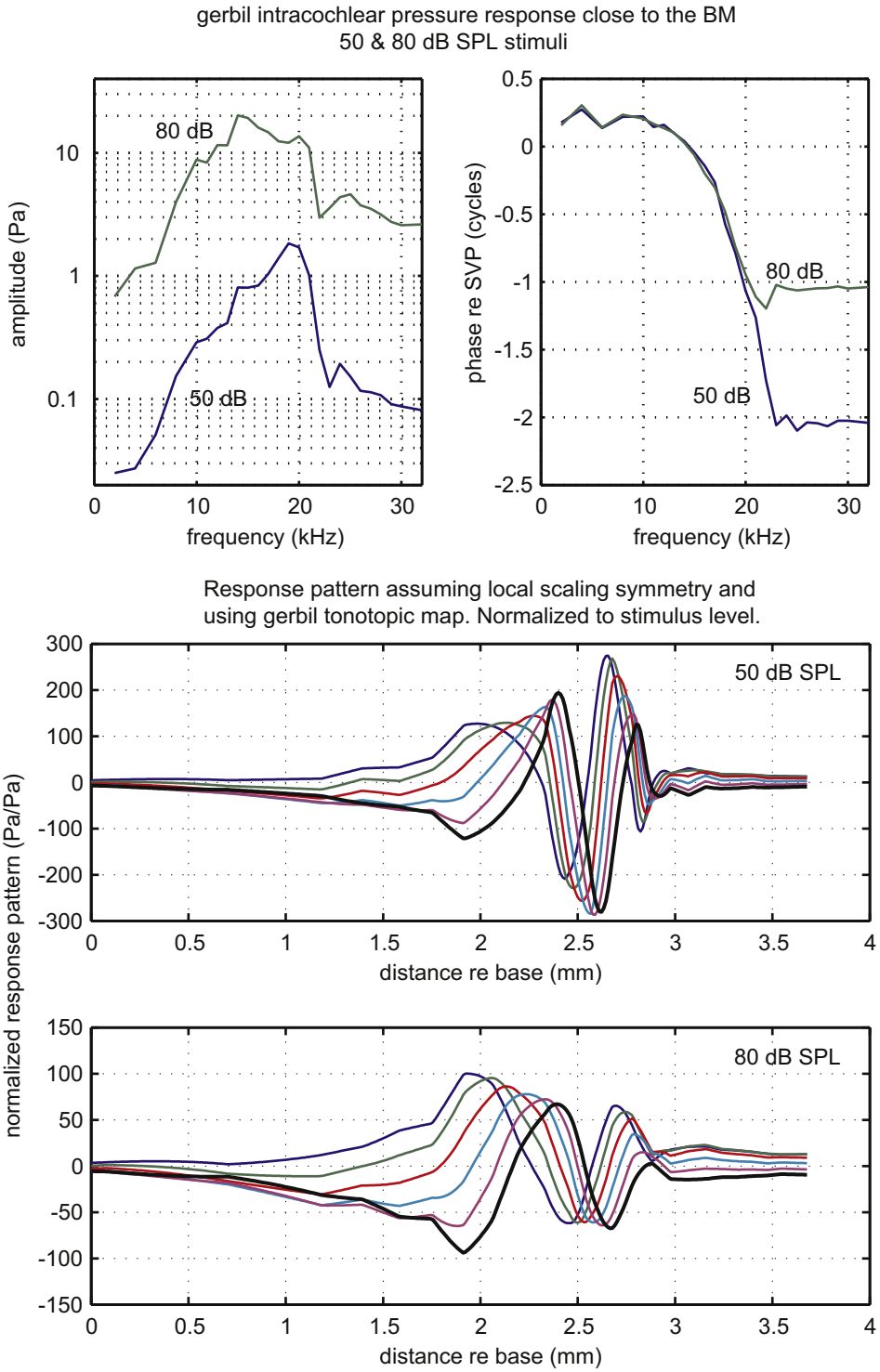

Fig. 6. Pressure close to the BM measured by Olson in gerbil. Upper panels show amplitude and phase as a function of frequency. In the lower two panels the data are replotted as the response pattern, assuming scaling symmetry and using the tonotopic map.

compliance measurements of Békésy. Using the left *y*-axis, Fig. 8A shows Békésy's results from his pages 476 and 510. To recast these as a compliance requires dividing by 100 Pa (the pressure stimulus for 1 cm of water) and dividing by 1 mm (the distance over which each volume measurement was made). Converting to SI units give the area compliance reported on the right hand y-axis. The area compliance is a number that is used directly in some cochlear models (e.g. Zwislocki, 1965). Many other cochlear models, rather than area/pressure, use displacement/pressure or its inverse. To present the compliance data in this form it is reasonable to approximate the displaced area as the BM width × the displacement height/2. Fig. 8B is derived in that way from Fig. 8A, and it is plotted as the inverse, to give stiffness (Pa/m) rather than compliance. In Fig. 8B gerbil has been included and several other animals not carried along – from now on we show gerbil (red), guinea pig (blue) and human (black). In some animals the BM has

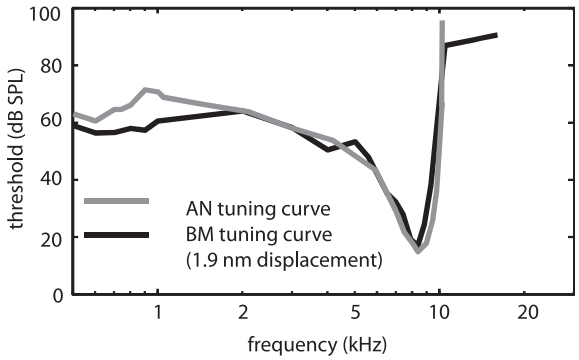

Fig. 7. Results from Ruggero et al. (2000) demonstrated the similarity between BM and AN tuning in the cochlear base.

a pronounced longitudinal width variation (a factor of five in human and water buffalo, Tiedemann, 1970), whereas in others (gerbil, Plassman et al., 1987, guinea pig, Fernandez, 1952) the width varies very little. The degree of width variation impacts the longitudinal variation in Fig. 8B compared to Fig. 8A. The gerbil data in Fig. 8B are from point stiffness measurements from two groups, Naidu and Mountain (1998) and Emadi et al. (2004). Point stiffness is measured and reported in N/m, with the point being a blunt needle, of diameter 10 μm (Naidu and Mountain) or 25 μm (Emadi et al.) To get to Pa/m, a simple (but incorrect) way would be to merely divide by the area of the probe tip. However, the BM is composed of radial fibers of collagen, and this anatomy asks to be treated as a beam (more on this is in the "Diversions" section below). With this in mind, a simple (but incorrect) way to go from N/m to Pa/m would be to assume that the point stiffness force was distributed over the whole beam. Then to get Pa/m stiffness (we'll refer to it as S_Pa/m) one would simply divide the N/m stiffness (S_N/m) by (tip width × BM width). The proper way to go from S_N/m to S_Pa/m is with a beam model as was developed in this context by Gummer et al. (1981). Here we simply state the answer for a centered probe: As long as the probe tip is substantially narrower than the width of the BM, S_Pa/m ~3.75(S_N/m)/(tip width × BM width) when the beam's edges are clamped, and S_Pa/m ~ 2.5(S_N/m)/(tip width × BM width) when the beam's edges are simply supported. Thus, doing the incorrect beam-based calculation above would introduce an error of a factor of ~3, and we can think of the factors of 3.75 or 2.5 as "correction factors." If the probe is *not* very small compared to the width of the BM, the correction factor is reduced. Using a correction factor of 3, and the known BM and tip width, the S_N/m data of Naidu and Mountain and Emadi et al. were recast as S_Pa/m to be included in Fig. 8B. In Fig. 8C the same results are replotted with the *x*-axis changed to percent of the cochlear length. More data are also included in the plot, because stiffness has been measured in the base of the gerbil and guinea pig cochlea in several ways. The Dong and Olson (2009)

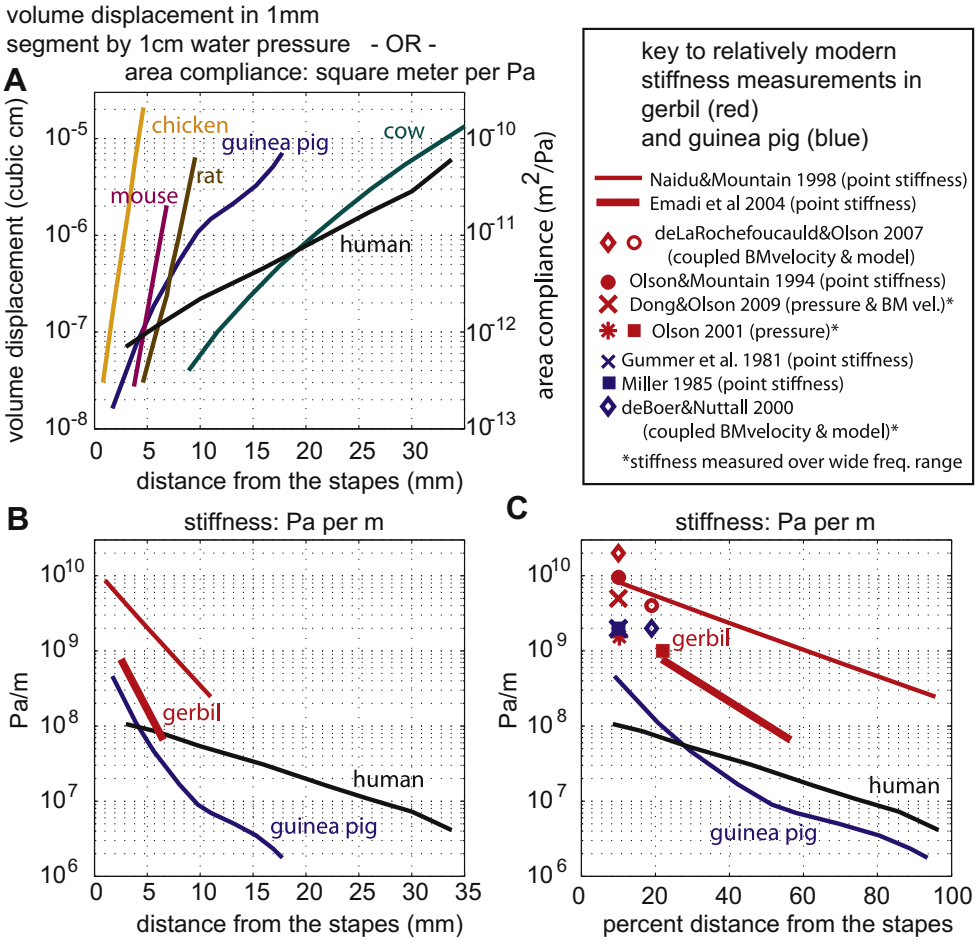

Fig. 8. Basilar membrane compliance and stiffness as a function of location from stapes. (A) Data from Békésy. (B) Stiffness replotted as Pa/m. Guinea pig and human data derived from panel A. Gerbil results derived from more recent point stiffness measurements. (C) Same as B except *x*-axis is percent distance from stapes, and additional basal measurements of stiffness included.

results were measured in vivo, at acoustic pressures of moderate value, and are the most direct. The de Boer and Nuttall (2000) and de La Rochefoucauld and Olson (2007) values were found by combining motion measurements with a cochlear 3-D box model. (The most basal deLaRochefoucauld and Olson value is rough, because the gerbil's very basal anatomy is not well approximated by a box model.) The Olson (2001) results were based on pressure measurements, with pressure gradients close to the BM used in a calculation to approximate BM motion. As noted with an asterisk in the key, some of these data sets cover an extensive range of auditory frequencies. The point stiffness measurements used probes that were much stiffer than the BM in all but the Emadi et al. measurement, for which the probe had stiffness comparable to that of the BM. Considering the guinea pig data, Békésy's basal values are about five times less stiff than the other basal guinea pig results, and the discrepancy is larger when comparing to the gerbil results. Even the modern gerbil measurements show substantial variability. Some of the discrepancy is due to the different methodologies and the approximations used to compare diverse data sets. While Békésy's guinea pig preparations were fresh, his technique would have likely have disrupted the cellular structure and this structure increases the stiffness measured at the BM by a factor of ~ two (Naidu and Mountain, 1998); see also Cooper (1999) and Eze and Olson (2011) for evidence for a substantial cellular contribution to stiffness.

In addition to quantitative measurements of volume compliance, Békésy made qualitative observations on the relative stiffness of intracochlear structures, and the beginning of his book's Ch. 12 describes the apparent relative stiffness of Hensen cells ("soft"), the reticular lamina ("a stiff covering plate from which hair cells hang down") and the tectorial membrane ("soft with great internal friction but rigid when touched with a needle moving at 200 Hz"). Modern measurements have provided significant quantitative advances, with measurements of tectorial membrane with micromachined probes (Freeman et al., 2003) and organ of Corti and tectorial membrane with atomic force microscopy (Scherer and Gummer, 2004; Gueta et al., 2006). The interpretation of these micromechanical measurements requires relatively advanced analysis – beyond a simple beam model. Modern observations of micromechanical motion in isolated and semi-intact preparations have both constrained and suggested new possibilities for what the motion of the organ of Corti is like in vivo (e.g. Karavitaki and Mountain, 2007; Nowotny and Gummer, 2011; Fridberger et al., 1998; Ulfendahl et al., 1989; Ghaffari et al., 2007).

3.3. Diversions

Békésy was remarkably thorough and prescient. However, a few of his conclusions were not correct and may have diverted progress.

Orthotropy of BM – Békésy reported that a probe caused an impression in the BM that was nearly circular near the probe. This implies that the membrane is isotropic, i.e., with the same stiffness in radial and longitudinal directions. However, the pectinate zone of the BM was named for the sharp radial lines that are so pronounced under the light microscope. These are the "resonating stretched strings" of the Helmholz theory. More recent studies establish that these lines are radial fibers of collagen II, imbedded in amorphous ground substance, without longitudinal cross links (Dreiling et al., 2002). So the microstructure indicates a highly orthotropic structure with low stiffness in the longitudinal direction. Some modelers remained with the isotropic membrane, because Békésy said so, and some finite element modelers use an isotropic membrane because it does not require such a fine mesh. The problem is that this yields a much slower high frequency roll off, which was not consistent with observations of BM motion. Voldrich (1983) pointed out: "The BM radial fibers keep the shape of deformation of the living membrane confined to a narrow transverse groove whereas a fixed membrane or one examined a few dozen minutes after death becomes deformed over a wide crater-shaped circular area." He suggested that Békésy did not use a sufficiently fresh preparation. However, it is difficult to believe that Békésy would make such an error. It should be noted that for a plate in bending, the ellipticity of the impression depends on the fourth root of the elasticity ratio, so for a ratio of radial to longitudinal elastic moduli of 100, the impression axes would have the ratio only around 3 – thus, the method of evaluation is not very sensitive to the thing being measured, and this might have contributed to Békésy's erroneous conclusion on isotropy. However, for the tectorial membrane he observed an impression consistent with the nearly radial collagen fibers.

Properties of tectorial membrane – Békésy reported that the tectorial membrane is very compliant for static displacement but almost rigid for a vibrating probe at 200 Hz. The recent measurement of the tectorial membrane by Freeman et al. (2003) indicates that in the range of 10–4000 Hz, there is only a modest increase in stiffness with frequency.

Property of endolymph – Békésy made the observation that the endolymph appeared to be similar to the vitrous humor. Recent workers have not reported this experience. From various sources, the protein content in percent by weight is roughly 0.05 for endolymph, 0.2 for perilymph, 1 for vitreous humor, and 1.8 for the tectorial membrane. So the endolymph is the least gel-like (Thalmann et al., 1992). Typically models use the properties of water for both endolymph and perilymph. Békésy further explored this by using a model with the scala tympani replaced by a gel and found no significant effect on the motion response. A gel has the same inertial properties as water, with the difference being in the damping. So this reinforces Békésy's point that the governing mechanics are the inertia of the fluid and the stiffness of the BM. This is further reinforced in the experimental model of Cancelli et al. (1985) that includes Reissner's membrane and the tectorial membrane. Increasing the viscosity of the endolymph by a factor of 10 only decreased the amplitude a bit. Also they found that making the tectorial membrane almost rigid had little effect on the BM response.

4. Theoretical cochlear models – a connection to modern mechanics

This tribute to Békésy's mechanics does not discuss several topics that, while key to our modern understanding, were not observed during his working lifetime. The prestin/OHC-motility/amplification/twitching-stereocilia story began in observations starting in the early 1970s, that continue to burst forth with adolescent energy. Similarly, cochlear emissions are a marvel first observed in the late 1970s, whose observation allows the non-invasive exploration of cochlear mechanics. Cochlear emissions appear to travel out of the cochlea as a combination of reverse cochlear traveling waves and pressure transmitted directly through the cochlear fluid (e.g., Shera and Guinan, 1999; Manley, 2001; Ren, 2004; Dong and Olson, 2008a,b). The relative proportion of these two exit routes is still uncertain and is of interest, because the exit route affects the interpretation of major characteristics of the emissions such as amplitude fine-structure and phase delay. Emissions are used to evaluate cochlear condition, and a better understanding of the emission process is a fascinating and clinically important research goal. References for these modern topics are in the book by Manley and Fay (2008).

Békésy measured passive mechanics, and the cochlea might be a unique sensory organ in that it "sort of" works even post mortem, displaying a traveling wave that peaks in the same general location

and with almost the same longitudinal variation in wavelength alive and just post mortem. Active cell-based mechanics modifies the response tremendously – in quantitative terms, producing sensory tissue motion of ~ a factor of a thousand larger than what obtains in a dead/passive cochlea. Perhaps this is not the remarkable observation however – after all, the difference between life and death is more than a factor of a thousand. Perhaps what is most remarkable is the way the living cells build upon the passive mechanical substrate – how much is unchanged, given how much is changed by active mechanics. In our final section we show results from two active cochlear models – going beyond Békésy for sure – to give brief examples of how modern theoretical cochlear mechanics has built on the foundation he gave us.

Passive cochlear traveling wave models have several basic forms, and are usually characterized by their dimensionality (1-D, 2-D or 3-D). The wave pattern emerges from these models by way of a WKB approximation or a finite element calculation (e.g., Steele and Taber, 1979), a transmission-line calculation (e.g., Peterson and Bogert, 1950), or an analytical approximation (Zwislocki, 1965). In all cases, the core result is a wave $\Psi(x,t) = \Psi_0 e^{i(\omega t - \int k(x)dx)}$ in which x is the longitudinal dimension. k, the wavenumber, is proportional to 1/wavelength and represents the curviness of the wave. In a mechanical wave k depends strongly on the compliance and in the cochlea, the wavelength decreases from base to apex due to the increasing compliance (Fig. 8) – thus, k is a strong function of x. As noted in the discussion of scale models above, and apparent in the presented traveling wave results, the passive traveling wave peaks where k begins its transition to large values (short wavelength). When cochlear activity is present the wave travels further, into regions with shorter wavelength, and can peak where the wavelength is only a few hundred micrometers in length. (As in our caveat on apical/basal differences above, we note that this pattern is not followed in the apex of the cochlea, where the wave seems to speed up again after passing through its best place (Rhode and Cooper, 1996). This mechanical behavior is also apparent in the reverse glides of ANs with CF < 750 Hz (Carney et al., 1999; Shera, 2001).)

There are many "active" cochlear models and they are designed to do different things – for example, understand the fundamental physics (e.g., de Boer, 1984; Steele, 1999), understand the emission process (e.g., Shera and Guinan, 1999), incorporate electro-mechanics realistically (Ramamoorthy et al., 2007; Mistrík et al., 2009), understand the relationship between AN tuning and BM tuning (e.g., Allen and Neely, 1992). Many models probe how cochlear amplification works: how it turns on at the right place/frequency (e.g., Hubbard, 1993) and how OHC electro-mechanics might operate to produce it (e.g., Geisler and Sang, 1995). In the below we briefly describe two models that provide two very different views of cochlear modeling.

4.1. Detailed macromechanical model with longitudinally coupled active force

The first model presented, the feed-forward/backward model of Steele and colleagues, adheres closely to the known mechanics, treating the fluid in 3-D and incorporating known anatomical/physical properties such as BM stiffness and width. The 3-D nature of the fluid was apparent to Békésy: the insensitivity of the BF to scala area in Békésy's physical models demonstrated that the significant behavior near BF is 3-D. In the cochlea the 3-D character is apparent in the rapid fall off in pressure with distance from the BM (e.g., Olson, 1999). In its passive form the model of Steele and colleagues was used to derive the cochlear map and passive tuning (Taber and Steele, 1981) – this can be contrasted to the many models that start with the map to derive a stiffness parameter. The active version of the model explores how active mechanics employs the existing anatomy to provide amplification (Lim and Steele, 2002; Yoon et al., 2011). OHC electromotility operates within the tilting architecture of the Deiters processes and OHCs to exert forces on downstream locations, as illustrated in Fig. 9.

The advantage of this distributed feed-forward/backward system is that its activation is controlled by a robust property of the traveling wave – its wavelength. In the model the OHC actuators are turned on all the time, yet in the long wavelength region, the actuators only have the effect of a small shift in the stiffness of the partition. The actuators become influential when they are in the vicinity of the best place where the wavelength of the traveling wave becomes short, because of the phase shift provided by the short wavelength and the longitudinal tilt of the cellular structure. Then the actuators have the effect of negative damping, providing amplification of the response by 40 dB or more. This provides tuned amplification, with the tuning mechanism operating in the wavelength, rather than the frequency domain. In the model, OHC forcing occurs cycle-by-cycle, independent of frequency, a reasonable first-order simplification (e.g., Frank et al., 1999; Rabbitt et al., 2009; Johnson et al., 2011; Dallos and Evans, 1995). BM velocity and pressure predictions from this model are roughly in agreement with measurements (Yoon et al., 2011). A similar wavelength-based tuning mechanism has been employed in several other models, for example (Geisler and Sang, 1995) and the relationship to time-delay models also explored (Zweig, 1976, 1991; Homer et al., 2011).

4.2. Time-domain nonlinear model

The second model, by Duifhuis, employs a time-domain model to study activity. Cochlear activity is included as a true nonlinearity, as opposed to the many models (including the one above) that employ a linearized-nonlinearity and are run in the frequency domain with the active component taking different values at different stimulus levels. A time-domain model is much more costly of computational time than a linearized frequency domain model and has the added complexity of a nonlinear activity parameter. Other simplifications are made, however. For example, the model presented here approximates the fluid in 1-D, and so far does not incorporate measured BM stiffness data. Stiffness is derived, based on the tonotopic map and a simple value for the mass per unit area. Thus, there are trade-offs. Two ways to improve the parameter selection are to use the currently available stiffness data, and to check wavelength responses and data. More realistic parameter selection has been explored for guinea pig (Schneider et al., 2000).

As is well known, nonlinear systems can behave in ways that are difficult to predict and time-domain models provide an essential check of the results of the frequency domain models (Duifhuis, 2012). For studying certain behaviors, such as distortion product

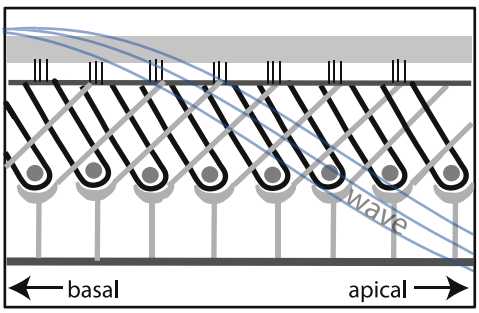

Fig. 9. Longitudinal anatomy of the organ of Corti. OHCs, outlined in black, are ~10 μm in diameter. Gray supporting structures are Deiters cells.

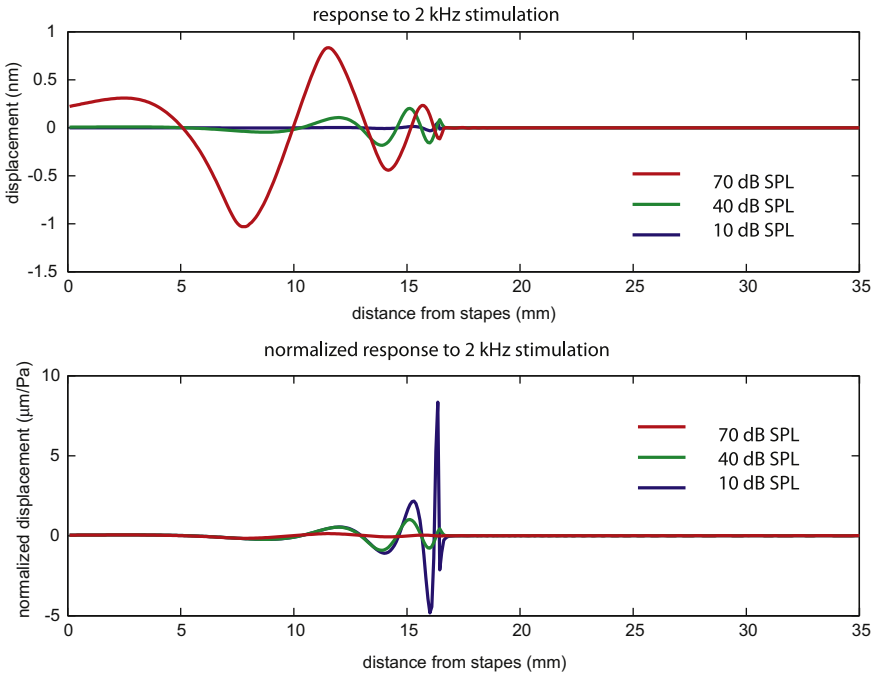

Fig. 10. Responses of a time-domain model to 2 kHz stimulation, with responses normalized to the stimulus level in the bottom panel.

and tone evoked emissions, for example Brass and Kemp's (1991) observation of otoacoustic emission during constant tone stimulation, nonlinear time-domain models are essential (Duifhuis and van den Raadt, 1997).

Fig. 10 shows the model's displacement response to a 2 kHz stimulus. Three stimulus levels are shown: 10, 40 and 70 dB SPL. In the lower panel the responses are normalized to the stimulus level. Many of the features of the traveling wave patterns in the experimental data are apparent. The normalized response maximum for 10 dB SPL stimulation is 50 times larger than the normalized response maximum at 70 dB SPL. Comparing the same longitudinal location, the wavelength lengthens just slightly as sound level increases. However, if you compare wavelength at the place of maximum, the higher stimulus curves peak further basal, where the wavelength is significantly longer. In the results here, the activity parameter reduced the resistance to almost zero. Reduction below zero (to negative resistance) results in oscillations that correspond to spontaneous otoacoustic emissions. In that case the damping is essentially nonlinear for small amplitudes, because increasing positive damping is required to achieve stability. In that case a local point behaves as an oscillator (Rayleigh or Van der Pol). If the cochlear parameters change smoothly, then the direct environment will not immediately dissipate the emission, and it will be transmitted into the fluid and leave the cochlea with a size that depends on the impedance match: transmission through the middle ear versus reflection at the stapes.

5. Closing

Békésy laid the groundwork for cochlear mechanics in his observations of the traveling wave, and his detailed and quantitative measurements on physical properties. In this contribution we have emphasized modern measurements that are closely related to Békésy's. Comparing to Békésy's time, the huge step forward in the field of cochlear mechanics has been the discovery and subsequent exploration of cochlear activity. This activity works within the framework of passive mechanics and the observations of Békésy are still our foundation – the roof continues to rise. In writings about Békésy by his contemporaries a theme is his love of art and of beauty (Ratlif, 1976). His Biographical Memoir recalls that Békésy wrote that once he saw the beauty of the cochlear anatomy, there was no going back. Békésy wrote in his 1961 (Békésy, 1961) Nobel lecture that he most appreciated great art that used nature as a source of creativity, and this led him to the realization that observing nature was also the source of scientific creativity. As a scientist he sought to uncover the beauty of the cochlea. We are fortunate to have had such an inspired and inspiring founder.

Acknowledgments

The authors are grateful to the Hearing Research editors, Barbara Canlon and special editor Peter Dallos, for inviting us to participate in the Békésy tribute issue, and to the reviewer for constructive comments. Tianying Ren, Marcel Van der Heijden, Philip Joris, William Rhode and Mario Ruggero generously contributed data. Thanks to Chris Shera for assistance with the concept of scaling symmetry. This work was funded in part by grants from the NIH NIDCD (R01DC00791004 and R01DC003130).

References

Allen, J.B., Neely, S.T., 1992. Micromechanical models of the cochlea. Phys. Today, 40–47.
Békésy, G., 1928. Zur Theorie des Hörens; die Schwingungsform der Basilarmembran. Phys. Zeits. 29, 793–810.
Békésy, G., 1960. Experiments in Hearing. McGraw-Hill, New York.
Békésy, G., December 11, 1961. Concerning the pleasures of observing, and the mechanics of the inner ear. Nobel Lect.
Brass, D., Kemp, D.T., 1991. Time-domain observation of otoacoustic emissions during constant tone stimulation. J. Acoust. Soc. Am. 90, 2415–2427.
Brownell, W.E., Bader, C.R., Bertrand, D., Ribaupierre, Y.D., 1985. Evoked mechanical responses of isolated cochlear outer hair cells. Science 227, 194–196.
Cancelli, C., D'Angelo, S., Masili, M., Malvano, R., 1985. Experimental results in a physical model of the cochlea. J. Fluid Mech. 153, 361–388.
Carney, L.H., 1994. Spatiotemporal encoding of sound level: models for normal encoding and recruitment of loudness. Hear. Res. 76, 31–44.
Carney, L.H., McDuffy, M.J., Shekhter, I., 1999. Frequency glides in the impulse responses of auditory-nerve fibers. J. Acoust. Soc. Am. 105, 2384–2391.

Chen, F., Zha, D., Fridberger, A., Zheng, J., Choudhury, N., Jacques, S., Wang, R.K., Shi, X., Nuttall, A.L., 2011. A differentially amplified motion in the ear for near-threshold sound detection. Nat. Neurosci. 14, 770–775.
Cooper, N.P., 1999. Radial variation in the vibrations of the cochlear partition. In: Wada, H., Takasaka, T.I.K., Ohyama, K., Koike, T. (Eds.), Proceedings of the International Symposium on Recent Developments in Auditory Mechanics. World Scientific, Sendai, Japan, pp. 109–115.
Cooper, N.P., Rhode, W.S., 1992. Basilar membrane mechanics in the hook region of cat and guinea pig cochlea: sharp tuning and nonlinearity in the absence of baseline shifts. Hear. Res. 63, 163–190.
Corti, A., 1851. Recherches sur l'organe de l'ouie des mammifères. Z. Wiss. Zool. 3
Dallos, P., Cheatham, M.A., 1971. Travel time in the cochlea and its determination from cochlear-microphonic data. J. Acoust. Soc. Am. 49, 1140–1143.
Dallos, P., Evans, B.N., 1995. High-frequency motility of outer hair cells and the cochlear amplifier. Science 267, 2006–2009.
de Boer, E., 1984. Auditory physics. Physical principles in hearing theory. Phys. Rep. 105, 141–226.
de Boer, E., Nuttall, A.L., 2000. The mechanical waveform of the basilar membrane III. Intensity effects. J. Acoust. Soc. Am. 107, 1497–1507.
de La Rochefoucauld, O., Olson, E.S., 2007. The role of organ of Corti mass in passive cochlear tuning. Biophys. J. 93, 3434–3450.
Dong, W., Cooper, N.P., 2006. An experimental study into the acousto-mechanical effects of invading the cochlea. J. Roy. Soc. Interf. 3, 561–571.
Dong, W., Olson, E.S., 2008a. Supporting evidence for reverse cochlear traveling waves. J. Acoust. Soc. Am. 123, 222–240.
Dong, W., Olson, E.S., 2008b. The roles of compression and traveling wave pressures in the transmission of sound out of the gerbil cochlea. In: Cooper, N.P., Kemp, D.T. (Eds.), Concepts and Challenges in the Biophysics of Hearing. World Scientific Press, Keele, UK, pp. 27–33.
Dong, W., Olson, E.S., 2009. In vivo impedance of the gerbil cochlear partition at auditory frequencies. Biophys. J. 97, 1233–1243.
Dreiling, F.J., Henson, M.M., Henson Jr., O.W., 2002. The presence and arrangement of type II collagen in the basilar membrane. Hear. Res. 166, 166–180.
Duifhuis, H., 2012. Introduction to a Time Domain Analysis of the Nonlinear Cochlea. Springer.
Duifhuis, H., van den Raadt, M.P.M.G., 1997. Usefulness of the nonlinear residual response method. In: Lewis, E.R., Long, G.F., Lyon, R.F., Narins, P.M., Steele, C.R., Hecht-Poinar, E. (Eds.), Diversity in Auditory Mechanics. World Scientific, pp. 226–232.
Eldredge, D.H., Miller, J.D., Bohne, B.A., 1981. A frequency-position map for the chinchilla cochlea. J. Acoust. Soc. Am. 69, 1091–1095.
Emadi, G., Richter, P.C., Dallos, P., 2004. Stiffness of the gerbil basilar membrane: radial and longitudinal variations. J. Neurophysiol. 91, 474–488.
Eze, N., Olson, E.S., 2011. Basilar membrane velocity in a cochlea with a modified organ of Corti. Biophys. J. 100, 858–867.
Fernandez, C., 1952. Dimensions of the cochlea (guinea pig). J. Acoust. Soc. Am. 24, 519–523.
Frank, G., Hemmert, W., Gummer, A.W., 1999. Limiting dynamics of high-frequency electromechanical transduction of outer hair cells. Proc. Natl. Acad. Sci. U. S. A. 96, 4420–4425.
Freeman, D.M., Abnet, C.C., Hemmert, W., Tsai, B.S., Weiss, T.F., 2003. Dynamic material properties of the tectorial membrane: a summary. Hear. Res. 180, 1–10.
Fridberger, A., Flock, A., Ulfendahl, M., Flock, B., 1998. Acoustic overstimulation increases outer hair cell Ca^{2+} concentrations and causes dynamic contractions of the hearing organ. Proc. Natl. Acad. Sci. U. S. A. 95 (12), 7127–7132.
Geisler, C.D., Sang, C., 1995. A cochlear model using feed-forward outer-hair-cell forces. Hear. Res. 86, 132–146.
Ghaffari, R., Aranyosi, A.J., Freeman, D.M., 2007. Longitudinally propagating traveling waves of the mammalian tectorial membrane. Proc. Natl. Acad. Sci. U. S. A. 104, 16510–16515.
Greenwood, D.D., 1990. A cochlear frequency-position function for several species – 29 years later. J. Acoust. Soc. Am. 87, 2592–2605.
Gueta, R., Barlam, D., Shneck, R.Z., Rousso, I., 2006. Measurement of the mechanical properties of isolated tectorial membrane using atomic force microscopy. Proc. Natl. Acad. Sci. U. S. A. 103, 14790–14795.
Guinan, J.J., Lin, T., Cheng, H., 2005. Medial-olivocochlear-efferent inhibition of the first peak of auditory-nerve responses: evidence for a new motion within the cochlea. J. Acoust. Soc. Am. 118, 2421–2433.
Gummer, A.W., Johnstone, B.M., Armstrong, N.J., 1981. Direct measurements of basilar membrane stiffness in the guinea pig. J. Acoust. Soc. Am. 70, 1298–1309.
Hasse, C., 1867. Die Schnecke der Vögel. Z. Wiss. Zool. 17
Held, H., 1926. Die Cochlea der Sauger und der Vogel, ihre Entwickhlung und ihr Bau. In: Handbuch der normalen und pathologischen Physiologie, Reception-sorgnne I. Springer, Berlin.
Helmholtz, H.L.F., 1885. On the Sensations of Tone. Dover, New York.
Homer, M., Szalai, R., Champneys, A., Epp, B., 2011. Comparing longitudinal coupling and temporal delay in a transmission line model of the cochlea. In: Shera, C.A., Olson, E.S. (Eds.), What Fire Is in Mine Ears. Proceedings of the 11th International Mechanics of Hearing Workshop, pp. 625–631.
Hubbard, A., 1993. A traveling-wave amplifier model of the cochlea. Science 259, 68–71.
Johnson, S.L., Beurg, M., Marcotti, W., Fettiplace, R., 2011. Prestin-driven cochlear amplification is not limited by the outer hair cell membrane time constant. Neuron 70, 1143–1154.
Joris, P.X., Van de Sande, B., Louage, D.H., van der Heijden, M., 2006. Binaural and cochlear disparities. Proc. Natl. Acad. Sci. U. S. A. 103, 12917–12922.
Kapuria, S., Steele, C.R., Puria, S., 2011. Mechanics of the unusual basilar membrane in gerbil. In: Shera, C.A., Olson, E.S. (Eds.), What Fire Is in Mine Ears. Proceedings of the 11th International Mechanics of Hearing Workshop, pp. 333–339.
Karavitaki, K.D., Mountain, D.C., 2007. Evidence for outer hair cell driven oscillatory fluid flow in the tunnel of Corti. Biophys. J. 92, 3284–3293.
Kemp, D.T., 1978. Stimulated acoustic emissions from within the human auditory system. J. Acoust. Soc. Am. 64, 1386–1391.
Kiang, N.Y.S., Moxon, E.C., 1973. Tails of tuning curves of auditory-nerve fibers. J. Acoust. Soc. Am. 55, 620–630.
Kiang, N.Y.S., Watanabe, T., Thomas, E.C., Clark, L.F., 1965. Discharge Patterns of Single Fibers in the Cat's Auditory Nerve. Research Monographs 35. M.I.T. Press, Cambridge, MA.
Kidd, R.C., Weiss, T.F., 1990. Mechanisms that degrade timing information in the cochlea. Hear. Res. 49, 181–208.
Kim, D.O., Molnar, C.E., 1979. A population study of cochlear nerve fibers: comparison of the spatial distribution of average-rate and phase-locking measures of responses to single tones. J. Neurophysiol. 42, 16–30.
Kölliker, A., 1852. Mikroskopische Anatomie oder Gewebelehre des Menschen. Leipzig.
Kolmer, W., 1909. Histologische Studien am Labyrinth. Arch. Mikroskop. Anat. 74
Kolston, P.J., 2000. The importance of phase data and model dimensionality to cochlear mechanics. Hear. Res. 145, 25–36.
Lim, K.M., Steele, C.R., 2002. A three-dimensional nonlinear active cochlear model analyzed by the WKB-numeric method. Hear. Res. 170, 190–205.
Manley, G.A., 2001. Evidence for an active process and a cochlear amplifier in nonmammals. J. Neurophysiol. 86, 541–549.
Manley, G.A., Fay, R.R. (Eds.), 2008. Active Processes and Otoacoustic Emissions in Hearing. Springer Handbook of Auditory Research, vol. 30.
Miller, C.E., 1985. Structural implications of basilar membrane compliance measurements. J. Acoust. Soc. Am. 77, 1465–1474.
Mistrík, P., Mullaley, C., Mammano, F., Ashmore, J., 2009. Three-dimensional current flow in a large-scale model of the cochlea and the mechanism of amplification of sound. J. Roy. Soc. Interf. 6, 279–291.
Müller, M., 1996. The cochlear place-frequency map of the adult and developing Mongolian gerbil. Hear. Res. 94, 148–156.
Müller, M., Hoidis, S., Smolders, J.W.T., 2010. A physiological frequency-position map of the chinchilla cochlea. Hear. Res. 268, 184–193.
Naidu, R.C., Mountain, D.C., 1998. Measurements of the stiffness map challenge a basic tenet of cochlear theories. Hear. Res. 124, 124–131.
Narayan, S.S., Temchin, A.N., Recio, A., Ruggero, M.A., 1998. Frequency tuning of basilar membrane and auditory nerve fibers in the same cochlea. Science 282, 1882–1884.
Nowotny, M., Gummer, A.W., 2011. Vibration responses of the organ of Corti and the tectorial membrane to electrical stimulation. J. Acoust. Soc. Am. 130, 3852–3872.
Olson, E.S., 1999. Direct measurement of intracochlear pressure waves. Nature 402, 526–529.
Olson, E.S., 2001. Intracochlear pressure measurements related to cochlear frequency tuning. J. Acoust. Soc. Am. 110, 349–367.
Olson, E.S., Mountain, D.C., 1994. Mapping the cochlear partition's stiffness to its cellular architecture. J. Acoust. Soc. Am. 95, 395–400.
Peterson, L.C., Bogert, B.P., 1950. A dynamical theory of the cochlea. J. Acoust. Soc. Am. 22, 369–381.
Plassman, W., Peetz, W., Schmidt, M., 1987. The cochlea in gerbilline rodents. Brain Behav. Evol. 30, 82–101.
Rabbitt, R.D., Clifford, S., Breneman, K.D., Farrell, B., Brownell, W.E., 2009. Power efficiency of outer hair cell somatic electromotility. PLoS Comput. Biol. 5, 1–14.
Ramamoorthy, S., Deo, N.V., Grosh, K., 2007. A mechano-electro-acoustical model for the cochlea: response to acoustic stimuli. J. Acoust. Soc. Am. 121, 2758–2773.
Ratlif, F., 1976. Georg Von Bekesy (1899–1972): A Biographical Memoir. National Academy of Sciences, Washington, DC.
Ravicz, M.E., Slama, M.C.C., Rosowski, J.J., 2010. Middle-ear pressure gain and cochlear partition differential pressure in chinchilla. Hear. Res. 263, 16–25.
Ren, T., 2002. Longitudinal pattern of basilar membrane vibration in the sensitive cochlea. Proc. Natl. Acad. Sci. U. S. A. 99, 17101–17106.
Ren, T., 2004. Reverse propagation of sound in the gerbil cochlea. Nat. Neurosci. 7, 333–334.
Retzius, G., 1884. Das Gehörorgan der Wirbeltiere. Stockholm.
Rhode, W.S., 1978. Some observation on cochlear mechanics. J. Acoust. Soc. Am. 64, 158–176.
Rhode, W.S., 2007. Basilar membrane mechanics in the 6–9 kHz region of sensitive chinchilla cochleae. J. Acoust. Soc. Am., 2792–2804.
Rhode, W.S., Cooper, N.P., 1996. Nonlinear mechanics in the apical turn of the chinchilla cochlea in vivo. Audit. Neurosci. 3, 101–121.
Roaf, H.E., 1922. Analysis of sound waves by the cochlea. Philos. Mag. 43 (254), 349–354.
Robles, L., Ruggero, M.A., 2001. Mechanics of the mammalian cochlea. Physiol. Rev. 81, 1305–1352.
Ruggero, M.A., Narayan, S.S., Temchin, A.N., Recio, A., 2000. Mechanical bases of frequency tuning and neural excitation at the base of the cochlea: comparison of basilar-membrane vibrations and auditory nerve-fiber responses in chinchilla. Proc. Natl. Acad. Sci. U. S. A. 97, 1174–11750.
Scherer, M.P., Gummer, A.W., 2004. Impedance analysis of the organ of Corti with magnetically actuated probes. Biophys. J. 87, 1378–1391.

Schmiedt, R.A., Zwislocki, J.J., 1977. Comparison of sound-transmission and cochlear-microphonic characteristics in Mongolian gerbil and guinea pig. J. Acoust. Soc. Am. 61, 133–149.
Schneider, S., Pris, V.F., Schoonhoven, R., van Hengel, P.W.J., 2000. F1- versus F2-sweep group delays of distortion product otoacoustic emissions in the guinea pig; experimental results and theoretical predictions. In: Wada, H., Takasaka, T.I.K., Ohyama, K., Koike, T. (Eds.), Proceedings of the International Symposium on Recent Developments in Auditory Mechanics. World Scientific, Sendai, Japan, pp. 360–366.
Shera, C.A., 2001. Frequency glides in click responses of the basilar membrane and auditory nerve: their scaling behavior and origin in traveling-wave dispersion. J. Acoust. Soc. Am. 109, 2023–2034.
Shera, C.A., Guinan, J.J., 1999. Evoked otoacoustic emissions arise by two fundamentally different mechanisms: a taxonomy for mammalian OAEs. J. Acoust. Soc. Am. 105, 782–798.
Steele, C.R., 1999. Toward three-dimensional analysis of cochlear structure. J. Oto-Rhino-Laryngol. 61, 238–251.
Steele, C.R., Taber, L.A., 1979. Comparison of WKB and finite difference calculations for a two-dimensional cochlear model. J. Acoust. Soc. Am. 65, 1001–1006.
Taber, L.A., Steele, C.R., 1981. Cochlear model including three-dimensional fluid and four modes of partition flexibility. J. Acoust. Soc. Am. 70, 426–436.
Thalmann, I., Comegysa, T.H., Liua, S.Z., Itob, Z., Thalmann, R., 1992. Protein profiles of perilymph and endolymph of the guinea pig. Hear. Res. 63, 37–42.
Tiedemann, H., 1970. A new approach to theory of hearing. Acta Otolaryngol. Suppl. 227, 1–50.
Ulfendahl, M., Flock, Å, Khanna, S.M., 1989. A temporal bone preparation for the study of cochlear micromechanics at the cellular level. Hear. Res. 40, 55–64.
Van der Heijden, M., Joris, P.X., 2006. Panoramic measurements of the apex of the cochlea. J. Neurosci. 26 (44), 11462–11473.
Voldrich, L., 1983. Experimental and topographical morphology in cochlear mechanics. In: de Boer, E., Viergever, M.A. (Eds.), Cochlear Mechanics. Mechanics of Hearing. Delft University Press, Delft, The Netherlands, pp. 163–167.
Wegel, R.L., Lane, C.E., 1924. The auditory masking of one pure tone by another and its probable relation to the dynamics of the inner ear. Phys. Rev. 23, 266–285.
Wever, E.G., 1962. Development of traveling-wave theories. J. Acoust. Soc. Am. 34, 1319–1324.
Yoon, Y.J., Steele, C.R., Puria, S., 2011. Feed-Forward and feed-backward amplification model from cochlear cytoarchitecture: an interspecies comparison. Biophys. J. 100, 1–10.
Zheng, J., Shen, W., He, D.Z.Z., Long, K., Madison, L.D., Dallos, P., 2000. Prestin is the motor protein of cochlear outer hair cells. Nature 405, 149–155.
Zweig, G., 1976. Basilar Membrane Motion in Cold Spring Harbor Symposia on Quantitative Biology, vol. XL. Cold Spring Harbor Laboratory, Cold Spring Harbor, NY, pp. 619–633.
Zweig, G., 1991. Finding the impedance of the organ of Corti. J. Acoust. Soc. Am. 89, 1229–1254.
Zwislocki, J., 1965. Analysis of some auditory characteristics. In: Luce, R.D., Bush, R.R., Galanter, E. (Eds.), Handbook of Mathematical Psychology, vol. III. John Wiley, New York, pp. 1–97.